

# QUANTIFYING OCEAN COLOR IN THE NORTH ATLANTIC AND NORTH PACIFIC OCEANS

Phytoplankton, the microscopic plants that form the lowest level of the oceanic food chain, reveal their presence because of their chlorophyll and other pigments, which change the color of ocean waters. Quantitative observations of ocean color can be used to estimate the concentration of these pigments. The first such observations of ocean color on a global scale were provided by the Coastal Zone Color Scanner, which was fielded on the Nimbus-7 satellite in 1978. At the Applied Physics Laboratory, data from the Coastal Zone Color Scanner have been used to quantify the spatial and temporal variability of ocean color (specifically water reflectance) in the North Atlantic and North Pacific oceans at wavelengths ranging from 400 to 600 nm. In addition to that work, several other applications of ocean color data also demonstrate the wide variety of investigations that can benefit from ocean color data.

## INTRODUCTION

The color of ocean water varies as a result of variations in material suspended or dissolved in the water. In the open ocean, the primary constituents affecting ocean color are the phytoplankton, which are passively floating or weakly swimming minute plant life. Ocean waters with very low concentrations of phytoplankton appear blue in sunlight. As the phytoplankton concentration increases, the water color shifts toward green. One can use remote sensors to detect and quantify this color shift and to estimate the concentration of phytoplankton.

Many factors affect the concentration of phytoplankton; they include light, nutrients, currents, temperature, grazing by zooplankton (passively floating or weakly swimming animals), and vertical mixing of the water column as a result of cooling and storms. Since those influences vary spatially and temporally, the concentration of phytoplankton also exhibits a great deal of spatial and temporal variability. Consequently, remote sensors that can repeatedly survey large areas are needed to characterize the variability of phytoplankton in the oceans.

This paper discusses one of the primary sensors used to collect ocean color data, the Coastal Zone Color Scanner (CZCS), and provides several applications of ocean color data.

## THE COASTAL ZONE COLOR SCANNER

The vast majority of the ocean color data available today were collected by the CZCS, which was one of the sensor systems on the Nimbus-7 spacecraft and the first satellite-based scanner specifically designed to observe the ocean at visible wavelengths. It had the sensitivity and wavelengths needed to observe ocean color changes associated with variations in phytoplankton concentration. The CZCS was a proof-of-concept instrument and was designed to have a one-year lifetime. Fortunately, it

far outlived its design life and collected data from October 1978 through June 1986.

The CZCS measured upwelling light at 443, 520, 550, and 670 nm with a spatial resolution at nadir of 825 m. Since light is scattered by the atmosphere, the upwelling light measured by the CZCS contains atmospheric as well as oceanic contributions. To quantify ocean color, the atmospheric contribution—arising from Rayleigh and aerosol scattering—must be subtracted from the radiance measured by the CZCS. Since most of the light at the sensor results from atmospheric scattering,<sup>1</sup> this so-called atmospheric correction must be done accurately to obtain accurate estimates of the water-leaving radiance. After atmospheric correction of CZCS data, the so-called bio-optical algorithms are applied to estimate the concentration of phytoplankton pigments from the water-leaving radiances at 443, 520, and 550 nm.<sup>2</sup> The algorithms are empirical and provide a quantitative relationship between ocean color and phytoplankton pigment concentration.

Water-leaving radiances from the CZCS provide not only an estimate of phytoplankton concentration but also an estimate of the ocean optical clarity. Optical clarity can be estimated since, in open ocean waters, spatial and temporal variations in ocean optical properties are governed largely by spatial and temporal variations of the phytoplankton concentration. The specific optical clarity parameter generally derived is the diffuse attenuation coefficient at a wavelength of 490 nm,  $K(490)$ . The inverse of this coefficient is known as the optical depth, the distance that 490-nm light travels before being attenuated by a factor of  $e$  ( $e \approx 2.718$ ). The clearest ocean waters have an optical depth (at 490 nm) of about 40 m, and turbid waters have optical depths of 5 m or less. Because of such attenuation, the CZCS provides only near-surface estimates of phytoplankton concentration and optical attenuation. In



fact, 90% of the water-leaving radiance originates in the upper attenuation length of the water column.<sup>3</sup>

The foregoing data-processing steps—that is, the atmospheric correction and application of the algorithms to derive estimates of phytoplankton concentration and water clarity—and other processing steps not detailed here were applied to the entire CZCS data set by investigators from the Goddard Space Flight Center and the University of Miami.<sup>4</sup> The resulting data set has proved valuable in a wide variety of civilian and military research investigations, as will be discussed in the next section.

## APPLICATIONS OF OCEAN COLOR DATA

The CZCS data set provides the observations necessary to study a variety of phenomena. In this section, I will discuss in some detail the application of CZCS data to the study of spatial and temporal variability in phytoplankton concentration and to the quantification of ocean color in terms of water reflectance. The section will conclude with a sampling of other uses of ocean color data.

### Characterization of Phytoplankton Variability

The CZCS data set has provided the first global view of oceanic phytoplankton and the complex spatial and temporal variations in phytoplankton that result from variability in factors that affect phytoplankton growth. A particularly striking example of the temporal variability observed by the CZCS is the spring bloom in the North Atlantic Ocean.<sup>5</sup> The bloom can be understood by considering the situation in many high-latitude areas in the winter, when deep mixing of the near-surface waters occurs (often extending to hundreds of meters) and ambient light levels are relatively low. The seasonally low light levels, combined with deep mixing (which carries the phytoplankton to depths where little light penetrates), results in available light levels that are insufficient to support significant phytoplankton production. In the spring, heating of the upper water column and a decreased intensity of storms allows the water column to stabilize so that near-surface mixing penetrates to a depth of only a few tens of meters. The decrease in the mixed-layer depth (which allows phytoplankton to remain in the near-surface waters where more light is available), along with increased light levels and the abundance of nutrients brought to the surface by deep winter mixing, allows for rapid phytoplankton growth, the so-called spring bloom of phytoplankton. The spring bloom can be seen by comparing Figures 1 and 2, which show median phytoplankton concentrations for March and May as derived from a subset of the global CZCS database.<sup>4</sup> Those figures indicate that phytoplankton concentrations in the northern North Atlantic Ocean increase significantly during the spring as the amount of light the phytoplankton have available increases. For example, in the area south of Iceland, pigment concentrations during March are on the order of 0.15 mg/m<sup>3</sup>. By May, the pigment concentration in that region has increased to 0.40 mg/m<sup>3</sup> or greater, and many areas show concentrations in excess of 0.65 mg/m<sup>3</sup>.

This type of cycle, where phytoplankton growth is governed largely by seasonally changing light levels and mixed-layer depths, contrasts with the situation in many

low-latitude areas, where the primary factor limiting growth is the availability of nutrients. Such an area is the one near Bermuda, where in the summer the upper ocean is strongly stratified, with a median mixed-layer depth of about 20 m. During the summer, phytoplankton in these waters have an abundance of light, but the strongly stratified waters inhibit the renewal of nutrients through mixing. Consequently, nutrients in the near-surface waters become depleted and phytoplankton levels are quite low. During the fall, when mixing brings additional nutrients to the surface, phytoplankton levels in the near-surface waters increase. This type of seasonal phytoplankton growth cycle is illustrated by Figure 3, which shows results compiled from a seven-year time series of *in situ* data taken about fifteen miles southeast of Bermuda. The time series was used to infer the minimum, median, and maximum pigment concentrations that would be observed by a remote sensor<sup>3</sup> during each month of the year. The figure shows that phytoplankton levels in the near-surface waters are consistently low from May through September when nutrients limit phytoplankton growth. During the period of increased mixing (October through April), phytoplankton levels tend to be elevated and are quite variable compared with levels during the summer.

Between the two extremes of nutrient- and light-limited phytoplankton populations are those where limitations to growth vary seasonally. Moreover, spatial and temporal variability can also result from a variety of other causes, such as grazing by zooplankton, currents, changes in species composition, temperature variations, and upwelling (in which subsurface waters rise, bringing up additional nutrients). These temporal and spatial variations in the influences on phytoplankton growth result in considerable temporal and spatial variability in phytoplankton standing stocks. Studies of such variability have been greatly aided by the data collected by the CZCS. For example, CZCS data have been used for testing models that characterize the spring bloom of phytoplankton,<sup>6</sup> for characterizing phytoplankton blooms in the marginal ice zone,<sup>7</sup> for characterizing eddies,<sup>8</sup> and for studying upwelling events.<sup>9,10</sup>

### Quantification of Ocean Color Variability

The CZCS water-leaving radiance data at 443, 520, and 550 nm have been used in a study at APL to characterize the spatial and temporal variability of ocean color at wavelengths ranging from 400 to 600 nm.<sup>11</sup> In this study, ocean color is characterized in terms of the water reflectance,  $R$ , defined as  $\pi$  times the in-water ratio of the upwelling radiance to downwelling irradiance. Water reflectance is estimated using a model developed by Howard Gordon of the University of Miami.<sup>12</sup> Using the results of Gordon's Monte Carlo simulations of light propagation and making various approximations, one can derive the following approximate relationship:<sup>11,12</sup>

$$R(\lambda) = \frac{0.346b_b(\lambda)}{K(\lambda)},$$

where  $R(\lambda)$  is the reflectance at wavelength  $\lambda$ ,  $b_b(\lambda)$  is the backscattering coefficient, and  $K(\lambda)$  is the diffuse attenuation coefficient. The value of  $K(\lambda)$  is estimated



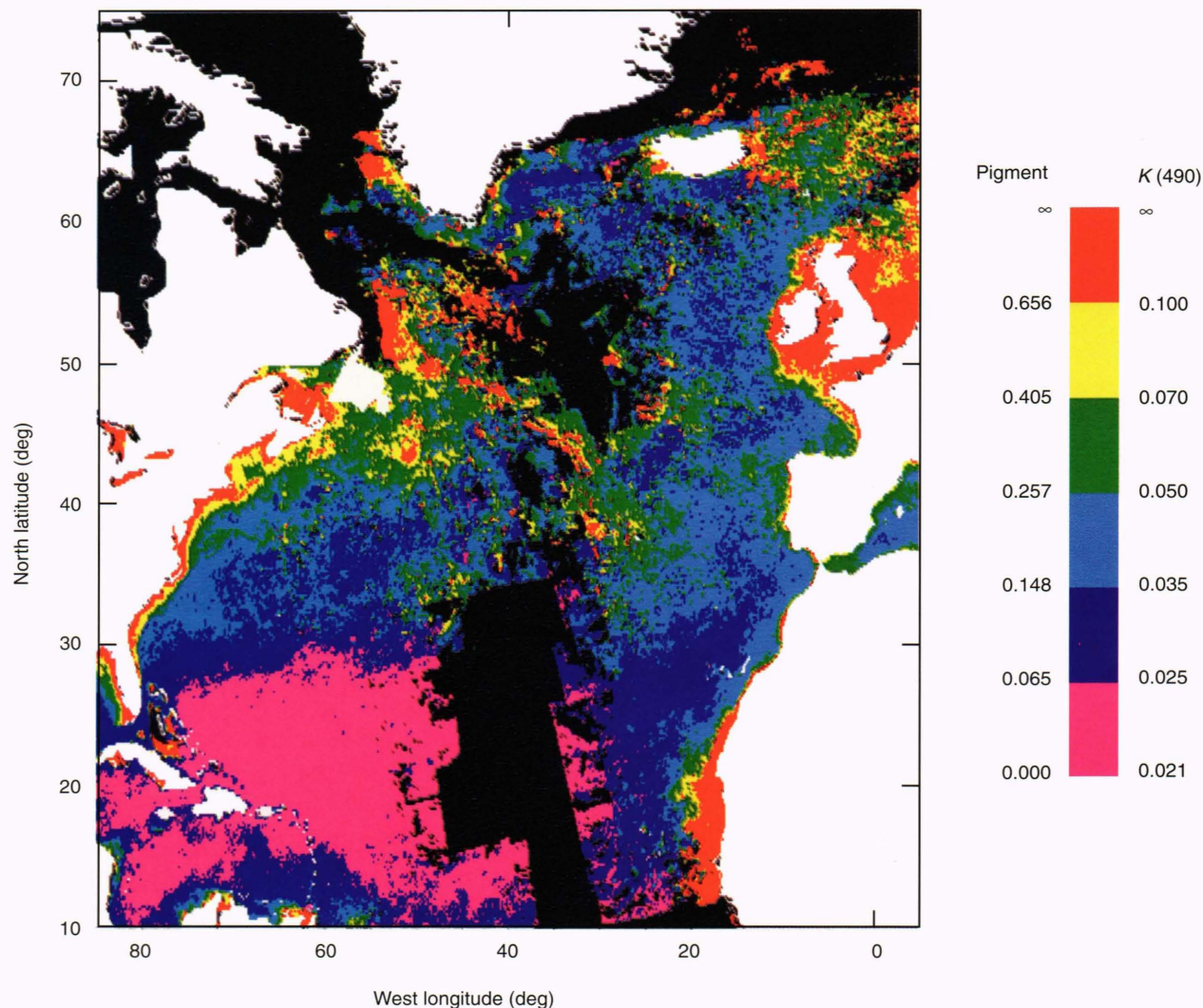


**Figure 1.** Median pigment concentration ( $\text{mg}/\text{m}^3$ ) and diffuse attenuation coefficient  $K(490)$  (in  $\text{m}^{-1}$ ) for March. Black denotes no data and white indicates land or ice.

using the ratio of water-leaving radiances at 443 and 550 nm and the Smith-Baker algorithm, which relates  $K(\lambda)$  and pigment concentration.<sup>15</sup> Backscattering is estimated from the magnitudes of the water-leaving radiances at 520 and 550 nm. Since the water-leaving radiances at 520 and 550 nm depend only weakly on pigment concentration, variations in the magnitude of the water-leaving radiances at those wavelengths result primarily from variations in backscattering rather than variations in pigment concentration. Backscattering is an important parameter to estimate, since the magnitude of backscatter can vary significantly even for a fixed pigment concentration.<sup>14</sup>

Sample reflectance results derived by applying Gordon's model to CZCS data are shown in Figures 4 through 6. Figure 4 shows reflectance curves typical for waters of the North Atlantic and North Pacific oceans. Curve 1 is a reflectance curve typical of clear-water areas where near-surface phytoplankton concentrations are low. Curve 2 is characteristic of moderately turbid waters, and curve 3 is characteristic of waters that are transitional

between those characterized by curves 1 and 2. Curve 4 is typical of very turbid waters where near-surface phytoplankton are abundant, and curve 5 is representative of very clear waters with particularly high reflectance. Figures 5 and 6 show where waters with reflectances that match the curves in Figure 4 can be found. (In this article, two reflectance curves are considered matching if at all wavelengths from 400 to 600 nm the difference in reflectance between the curves is less than or equal to one percent. February data used are from 1979, 1980, and 1981; August data are from 1979 and 1980.) As Figures 5 and 6 indicate, curve 1 of Figure 4 matches large areas in the southern portion of the region where clear waters occur. Curve 2 matches fairly large regions in the northern portion of the area where moderately turbid waters are found. Curve 3 falls between curves 1 and 2 and matches areas where water properties change from those characteristic of curve 1 to those characteristic of curve 2. Curve 4 matches northern and near-coastal areas where very turbid waters are encountered. Curve 5 matches



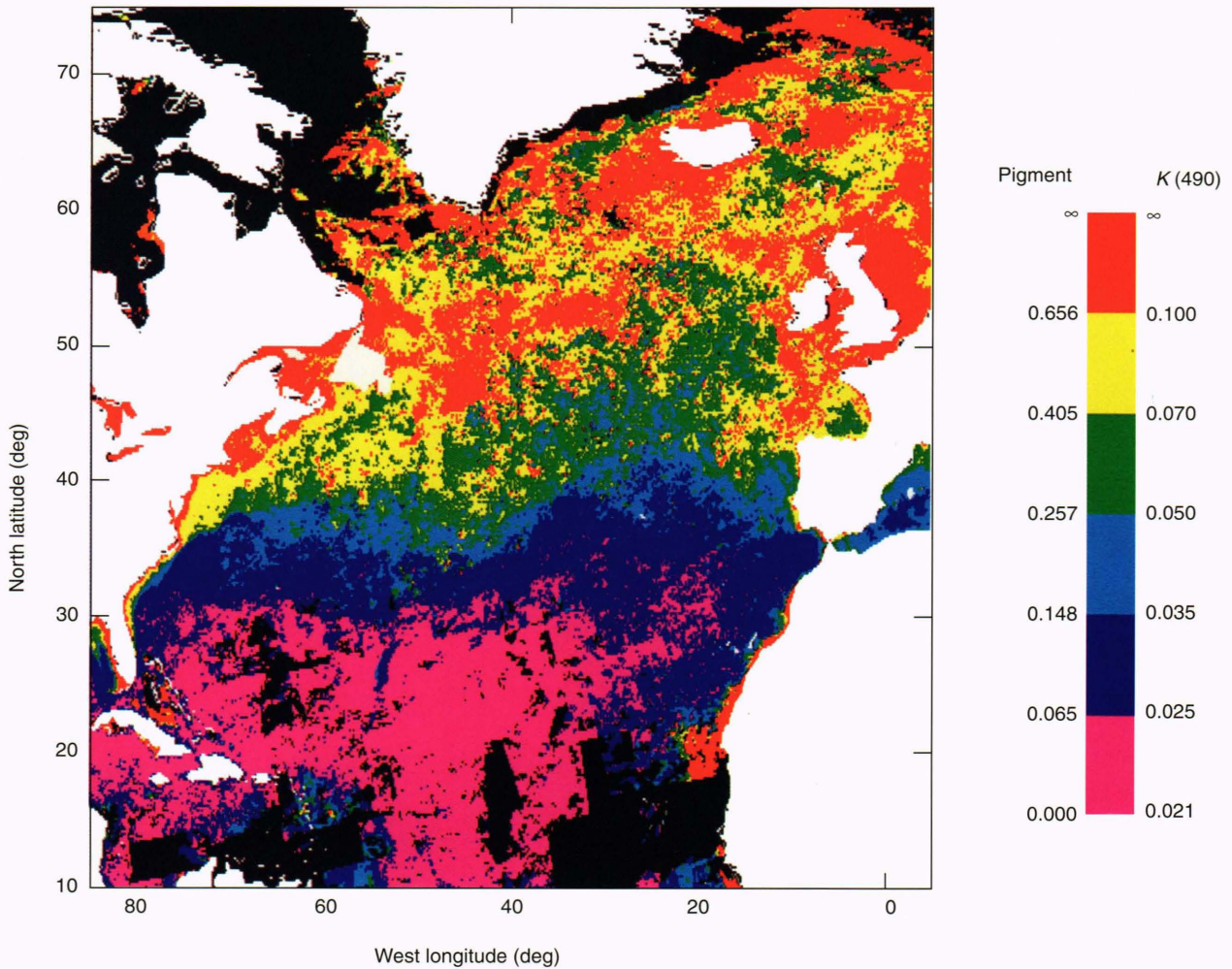


**Figure 2.** Median pigment concentration ( $\text{mg}/\text{m}^3$ ) and diffuse attenuation coefficient  $K(490)$  (in  $\text{m}^{-1}$ ) for May. Black denotes no data and white indicates land or ice.

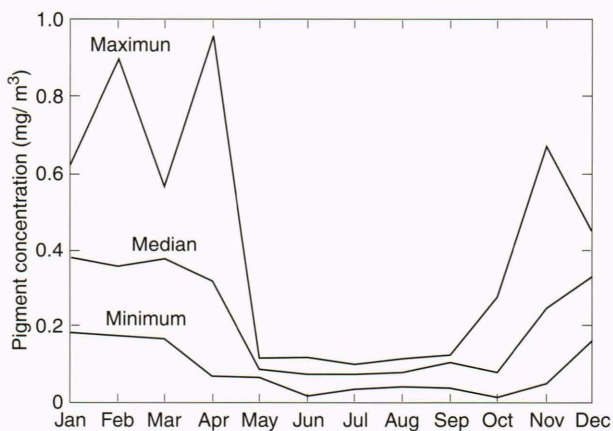


**Figure 3.** Minimum, median, and maximum pigment concentrations observed at station S near Bermuda (located at  $32^{\circ}10'N$ ,  $64^{\circ}30'W$ ) for each month of the year.

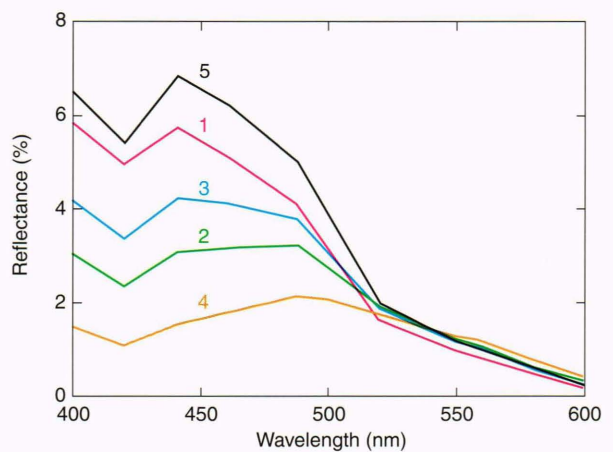


**Figure 4.** Reflectance curves characteristic of North Atlantic and North Pacific waters. Curve 1: Clear water with low phytoplankton concentrations. Curve 2: Moderately turbid water. Curve 3: Water transitional between waters characterized by curves 1 and 2. Curve 4: Very turbid water with abundant phytoplankton. Curve 5: Very clear water with high reflectance.



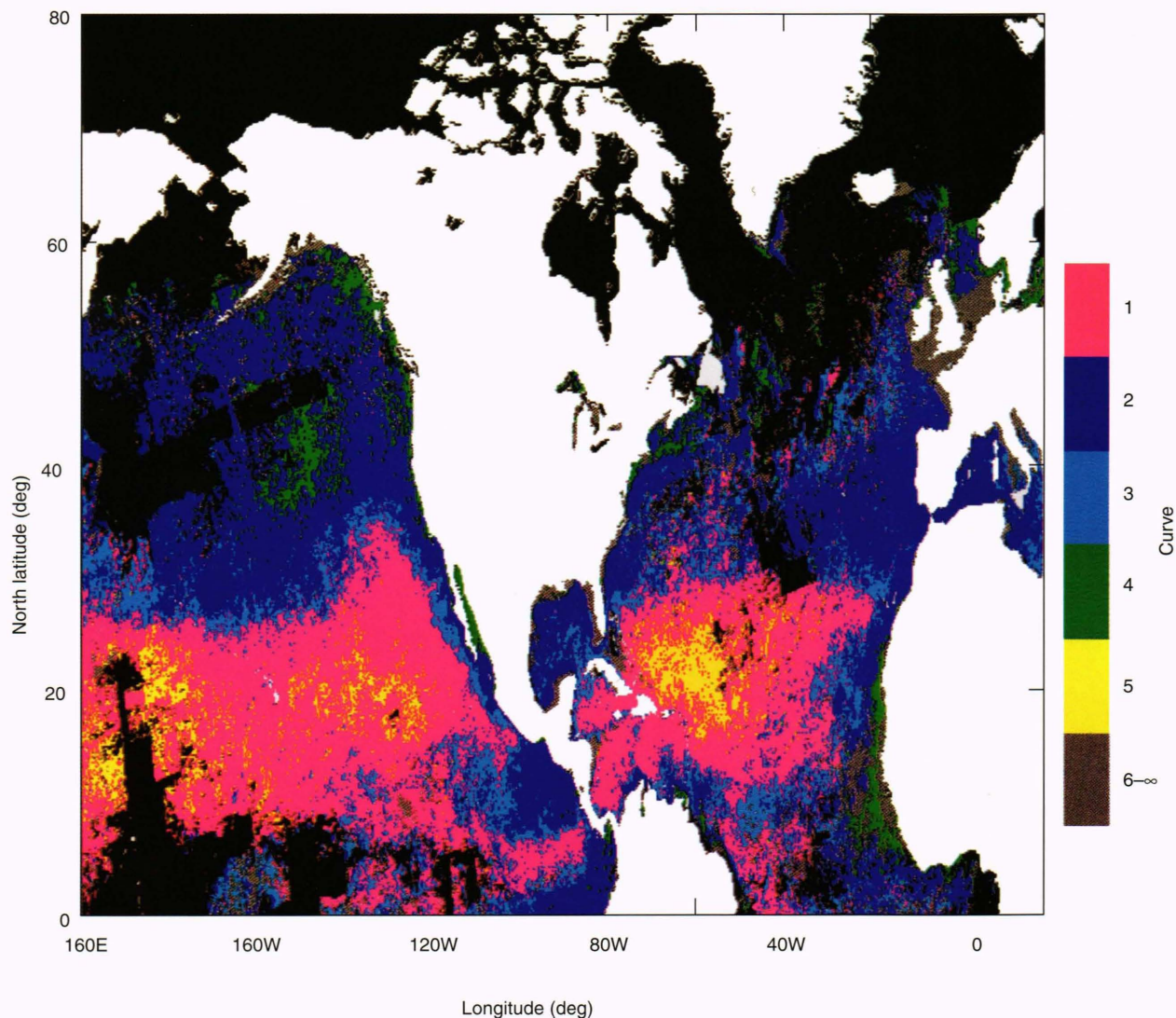


**Figure 5.** Map for February showing areas with reflectance that matches (to within  $\pm 1\%$ ) the reflectance curves shown in Figure 4. Black indicates no CZCS data and white denotes land or ice. Colors indicate the reflectance curve in Figure 4 that matches the water reflectance for that location in February. Gray areas are not matched by any of the curves in Figure 4.

areas where clear waters with relatively high reflectance occur. Areas not matched by any of the curves in Figure 4 are gray in Figures 5 and 6; reflectance curves matched by waters in the gray areas occur infrequently and for simplicity are not shown (10.4% of waters in the area shown are not matched by the five curves in Fig. 4).

Figures 5 and 6 illustrate the significant changes in phytoplankton concentrations and the consequent changes in ocean color that can occur from one season to another. For example, clear waters (characterized by reflectance curves 1 and 5) extend much farther north in August than in February, largely as a result of near-surface nutrient depletion that occurs during the summer when the strong stratification inhibits vertical mixing and nutrient replenishment. With the near-surface nutrient supply depleted, phytoplankton levels fall to low values and waters are quite clear and have a relatively high reflectance.

### Other Applications of CZCS Data

The applications I have noted comprise but a small sample of the many uses of CZCS data. We will turn now briefly to other civilian and military uses of CZCS data.

Since oceanic phytoplankton utilize significant amounts of carbon dioxide ( $\text{CO}_2$ ), one major use of ocean color data is in assessing the role phytoplankton play in the global carbon cycle.<sup>15</sup> Ocean color data provide a great deal of information about phytoplankton concentration, which in turn can be used to estimate  $\text{CO}_2$  consumption. But since 90% of the water-leaving radiance originates in the upper attenuation length (at most about 40 m), ocean color data provide only near-surface estimates of phytoplankton concentration.<sup>3,16</sup> Algorithms relating this near-surface biomass measurement to phytoplankton growth throughout the water column are used to assess the quantity of  $\text{CO}_2$  consumed by phytoplankton.



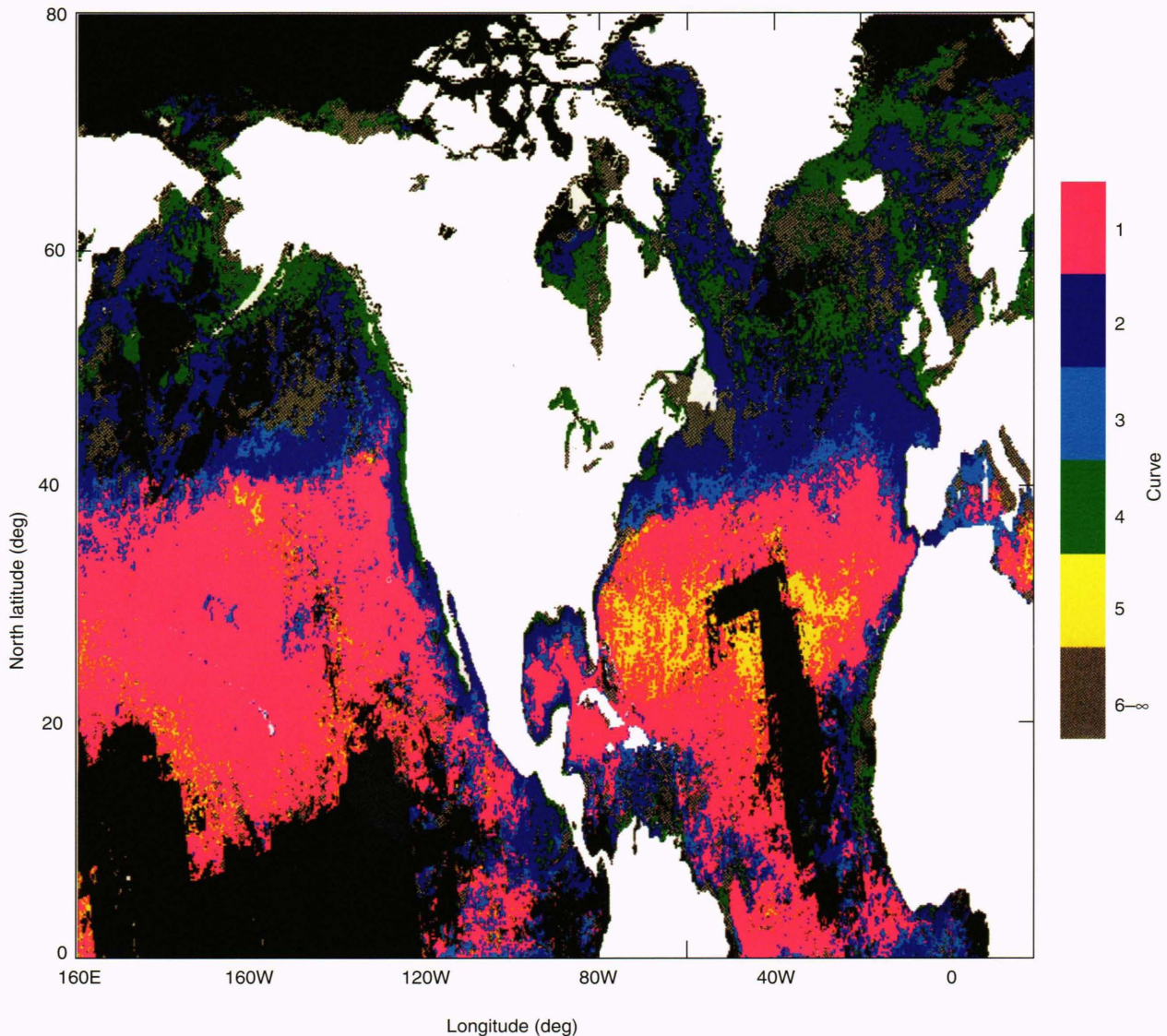


**Figure 6** Map for August showing areas with reflectance that matches (to within  $\pm 1\%$ ) the reflectance curves shown in Figure 4. Black indicates no CZCS data and white denotes land or ice. Colors indicate the reflectance curve in Figure 4 that matches the water reflectance for that location in August. Gray areas are not matched by any of the curves in Figure 4.

Another use of ocean color data is in locating fronts and tracking water masses such as river plumes and eddies. In this regard, ocean color sensors can augment the capability provided by satellite infrared sensors, which provide the means to distinguish water masses on the basis of temperature differences. Ocean color sensors can be useful in situations where surface heating has eliminated the near-surface temperature contrast between water masses but a color contrast still exists. Ocean color sensors also provide important ocean front observations in situations where atmospheric moisture is high.<sup>17</sup> When atmospheric moisture is high, the upwelling visible radiation can penetrate more readily than the infrared radiation, since absorption by water vapor is lower in the visible than in the infrared.

The ability to track oceanic fronts and eddies is useful for both civilian and military purposes. On the civilian side, tracking of fronts and eddies can aid in studies of

the dynamics of ocean currents and in biological oceanography. One of the most practical uses of the ability to locate ocean color fronts may be in the fishing industry; albacore tuna have been found to aggregate at ocean color fronts off the west coast of the U.S.<sup>18</sup> On the military side, fronts and eddies are significant for both acoustic and nonacoustic antisubmarine warfare. The large changes in sound velocity typically associated with water mass boundaries makes them important in underwater sound propagation. In addition, ocean optical clarity can change markedly in the vicinity of a front or eddy, resulting in substantial changes in the performance of optical detection systems.

Finally, other military applications of ocean color data can be found in mine warfare, submarine laser communications, and optical mapping of bathymetry in shallow areas.<sup>17</sup> In those applications, ocean color data can be used to estimate ocean optical properties and system



performance. For example, estimates of optical clarity can be used to judge the approximate depth to which communications to a submarine are reliable. Also, in the use of airborne lasers to map bathymetry, ocean optical data can provide information about the spatial and temporal variability of ocean optical properties. Such information can be used for survey planning to improve the efficiency and areal coverage of laser bathymetric surveys. For example, in many areas water clarity varies significantly with time. Ocean color data can be used to determine when waters are clearest and therefore provide the best conditions for an optical bathymetric survey.

## SUMMARY

The CZCS demonstrated that ocean color data are valuable for an exceptionally wide variety of applications, including location of areas likely to contain commercially valuable fish, assessment of the role of oceanic phytoplankton in the global carbon cycle, studies of phytoplankton spatial and temporal variability, studies of the dynamics of fronts and eddies, and assessment of the performance of antisubmarine warfare sensor systems. Because many of these applications require real-time data, the failure of the CZCS in 1986 represented a serious limitation to the application of ocean color data. Fortunately, the collection of remotely sensed ocean color data will resume in early 1994 with the fielding of the Sea-viewing Wide-Field-of-view Sensor (SeaWiFS). The SeaWiFS will measure the ocean color at more visible bands and with a higher signal-to-noise ratio than did the CZCS.<sup>19</sup> Moreover, improved atmospheric correction algorithms, sensor calibration methods, bio-optical algorithms (for relating ocean color to water contents including phytoplankton pigments), and a 100% daylight duty cycle (the CZCS only took selected imagery and had a duty cycle of less than 10%) will provide a higher-quality data set with better spatial and temporal coverage. SeaWiFS data will provide the information needed to accelerate the progress of research in the exceptionally wide variety of areas in which ocean color data can be applied.

## REFERENCES

- <sup>1</sup>Gordon, H. R., and Castano, D. J., "Coastal Zone Color Scanner Atmospheric Correction Algorithm: Multiple Scattering Effects," *Appl. Opt.* **26**, 2111-2122 (1987).
- <sup>2</sup>Gordon, H. R., Clark, D. K., Brown, J. W., Brown, O. B., Evans, R. H., et al., "Phytoplankton Pigment Concentrations in the Middle Atlantic Bight: Comparison of Ship Determinations and CZCS Estimates," *Appl. Opt.* **22**, 20-36 (1983).
- <sup>3</sup>Gordon, H. R., and Clark, D. K., "Remote Sensing Optical Properties of a Stratified Ocean: An Improved Interpretation," *Appl. Opt.* **19**, 3428-3430 (1980).
- <sup>4</sup>Feldman, G. C., Kuring, N., Ng, C., Esaias, W. E., McClain, C., et al., "Ocean Color—Availability of the Global Data Set," *EOS, Trans. Am. Geophys. Union* **70**, 634, 635, 640-641 (1989).
- <sup>5</sup>Esaias, W. E., Feldman, G. C., McClain, C. R., and Elrod, J. A., "Monthly Satellite-Derived Phytoplankton Pigment Distribution for the North Atlantic Ocean Basin," *EOS, Trans. Am. Geophys. Union* **67**, front cover and 835-837 (1986).

- <sup>6</sup>Wroblewski, J. S., Sarmiento, J. L., and Flierl, G. R., "An Ocean Basin Scale Model of Plankton Dynamics in the North Atlantic: 1. Solutions for the Climatological Oceanographic Conditions in May," *Global Biogeochem. Cycles* **2**, 199-218 (1988).
- <sup>7</sup>Sullivan, C. W., McClain, C. R., Comiso, J. C., and Smith, W. O., Jr., "Phytoplankton Standing Crops Within an Antarctic Ice Edge Assessed by Satellite Remote Sensing," *J. Geophys. Res.* **93**, 12,487-12,498 (1988).
- <sup>8</sup>Gordon, H. R., Clark, D. K., Brown, J. W., Brown, O. B., and Evans, R. H., "Satellite Measurement of the Phytoplankton Pigment Concentration in the Surface Waters of a Warm Core Gulf Stream Ring," *J. Marine Res.* **40**, 491-502 (1982).
- <sup>9</sup>Abbott, M. R., and Zion, P. M., "Satellite Observations of Phytoplankton Variability During an Upwelling Event," *Cont. Shelf Res.* **4**, 661-680 (1985).
- <sup>10</sup>McClain, C. R., Pietrafesa, L. J., and Yoder, J. A., "Observations of Gulf Stream-Induced and Wind-Driven Upwelling in the Georgia Bight Using Ocean Color and Infrared Imagery," *J. Geophys. Res.* **89**, 3705-3723 (1984).
- <sup>11</sup>Stark, V. L., with contributions from Gordon, H. R., "Variability of Reflectance as Inferred from CZCS Data," JHU/APL Report STD-R-2029 (1991).
- <sup>12</sup>Gordon, H. R., Brown, O. B., Evans, R. H., Brown, J. W., Smith, R. C., et al., "A Semianalytic Radiance Model of Ocean Color," *J. Geophys. Res.* **93**, 10,909-10,924 (1988).
- <sup>13</sup>Baker, K. S., and Smith, R. C., "Bio-optical Classification and Model of Natural Waters. 2," *Limnol. and Oceanogr.* **27**, 500-509 (1982).
- <sup>14</sup>Gordon, H. R., and Morel, A. Y., *Remote Assessment of Ocean Color for Interpretation of Satellite Visible Imagery: A Review*, Springer-Verlag, New York (1983).
- <sup>15</sup>Gower, J. F. R., "Potential Future Applications of Ocean Colour Sensing for Large Scale and Global Studies," *Adv. Space Res.* **9**, (7)39-(7)43 (1989).
- <sup>16</sup>Balch, W., Evans, R., Brown, J., Feldman, G., McClain, C., et al., "The Remote Sensing of Ocean Primary Productivity: Use of New Data Compilation to Test Satellite Algorithms," *J. Geophys. Res.* **97**, 2279-2293 (1992).
- <sup>17</sup>Hickman, G. D. (ed.), *Applications of Ocean Color to Naval Warfare*, Naval Oceanographic and Atmospheric Research Laboratory Report NOARL-BC-009-91-321 (1992).
- <sup>18</sup>Laur, R. M., Fiedler, P. C., and Montgomery, D. R., "Albacore Tuna Catch Distributions Relative to Environmental Features Observed from Satellites," *Deep-Sea Res.* **31**, 1085-1099 (1984).
- <sup>19</sup>McClain, C. R., Esaias, W. E., Barnes, W., Guenther, B., Endres, D., et al., *SeaWiFS Calibration and Validation Plan*, Vol. 3, NASA Technical Memorandum 104566 (1992).

## THE AUTHOR



VERNON L. STARK received a B. S. in physics from Colorado State University in 1977 and an M. S. in applied physics from The Johns Hopkins University in 1980. Mr. Stark joined APL in 1977 and has worked in a variety of areas including optical oceanography, physical oceanography, data analysis, and tactical simulation. His interests include optical oceanography, biological oceanography, and remote sensing.